*34th EPS Conference on Plasma Phys. Warsaw, 2 - 6 July 2007 ECA Vol.**31F**, P-5.089 (2007)*

Local Emission Profiles from Impurity Ions and Visible Bremsstrahlung in the TJ-II Stellarator

A. Baciero, B. Zurro, D. Rapisarda, D. Jiménez-Rey, F. Medina, J. Herranz, I. Pastor, C. Fuentes, J. Guasp, M. Liniers and the TJ-II team

Laboratorio Nacional de Fusión por Confinamiento Magnético, Asociación Euratom-CIEMAT para Fusión. Madrid, Spain

Introduction

An experimental system based on a rotating mirror and a monochromator is employed to obtain local emission profiles from TJ-II plasmas.[1] This system permits very precise selection of the spectral band. In a previous work,[2] we used this system to deduce Z_{eff} profiles from visible bremsstrahlung emission and we developed an in-house iterative method to deduce Z_{eff}. In this work, we replace that procedure with tomographic inversion based on minimising Fisher's information (Fisher inversion), which has already been employed in plasma analyses.[3,4] The local profiles obtained are allowed to be asymmetric in order to determine if emission depends on plasma side.

Experimental

Plasma emissions are reflected by a fast rotating hexagonal mirror (by Lincoln Laser, USA) to a ½ meter monochromator (by Acton Research, USA), that selects radiation wavelength from 200 to 800 nm with an spectral width of ~1.6 nm. Next, the light is registered using a photomultiplier (Model H9305-04 by Hamamatsu, Japan) and recorded by the TJ-II data acquisition system (Fig. 1(*a*)). This system is capable of obtaining a plasma emission profile (time interval ~ 1 ms, Fig. 2(*a*)) every 8 ms. The system is located near the NBI injector and it observes the plasma-NBI beam interaction area.

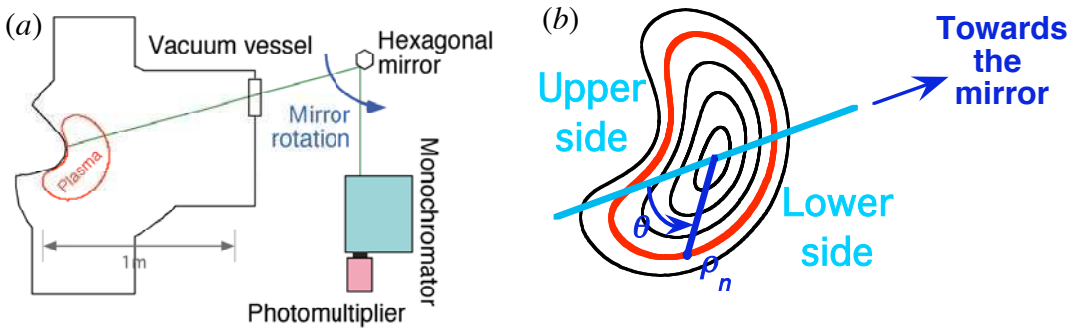

Fig. 1. (a) Sketch of the experimental set-up. (b) The TJ-II magnetic surfaces and the local coordinates used with the Fisher inversion method.

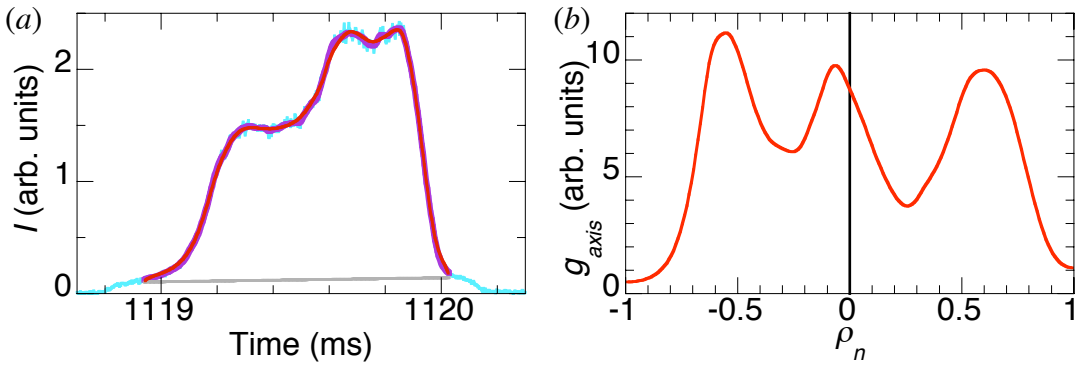

Fig. 2. (a) A single chord-integrated C V emission profile: original data (cyan), input data (purple), background (grey) and reconstructed chord-integrated profile with deduced local profile (red). (b) Deduced local emission profile.

A spectral survey was carried out in a previous work[2] over the monochromator range using a high-resolution spectrometer with a multi-channel detector. It was found that the spectral range between 522.5 - 525.5 nm is free of significant line emissions, and hence was chosen to measure visible bremsstrahlung profiles.

Data analysis

Once we have measured plasma chord-integrated emission, we need to know the relation between measurement time and spatial position. In order to do this, several steps are followed: *i*) Calculate the signal repetition frequency (signal autocorrelation) in order to find the relation between angle width and time interval; *ii*) Smooth the signal to reduce spurious noise (input data); *iii*) Determinate the profile chord-integrated profile edges, that are defined as positions where the profile second derivative changes its sign (edges values also define background value); and *iv*) determine the profile area that covers the width determined by the detector geometry and last closed magnetic surface position.

Next, we can perform the Fisher inversion method[3] with chord-integrated measurements. The Fisher method uses a non-linear regularization that minimizes $\int (g')^2/g$, where g is the local profile and g' its derivative. The Fisher solution profile tends to be flatter for lower values of g, where the signal-to-noise relation is poor. In our case, the local profile of g will depend on ρ_n (normalised magnetic radius) and θ, an angle defined by the geometry of observation (Fig 1(*b*)). Then, the local emission for a given position is:

$$g(|\rho_n|,\theta) = \left(\frac{1-\sin\theta}{2}\right) g_{axis}(-|\rho_n|) + \left(\frac{1+\sin\theta}{2}\right) g_{axis}(|\rho_n|) \qquad (1)$$

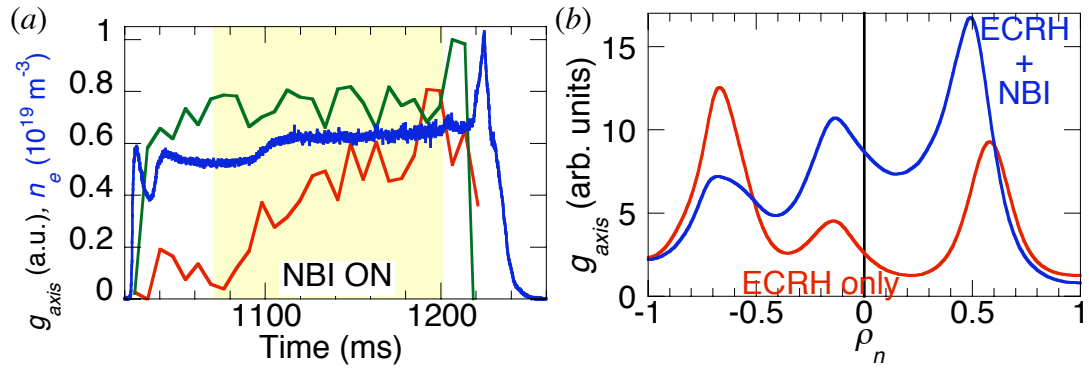

Fig. 3. (a) Evolution of C V central peak height (red) and non-central (green) in a NBI pulse. Electron density is also shown (blue). (b) He II profile changes during NBI heating.

Here g_{axis} is the local profile for the axis whose $\theta = \pm\pi/2$. This emission model allows distinguishing between the two plasma sides: if $g_{axis}(|\rho_n|) > g_{axis}(-|\rho_n|)$, then the lower side emits stronger than the upper side for same ρ_n.

Finally, we can deduce the Z_{eff} profile from the local visible bremsstrahlung profile when T_e and n_e profiles (Thomson Scattering diagnostic)[5] are measured:[6]

$$\varepsilon_\lambda = \xi(\lambda) n_e^2 Z_{eff}^{0.945} T_e^{-0.318} \qquad (2)$$

Here $\xi(\lambda)$ only depends on emission wavelength (λ).

Results and discussion

In Fig. 2, we show a C V (227.1 nm) profile fit for a TJ-II plasma heated with ECRH. We observe three peaks: one peak near the plasma centre and two peaks at $\rho_n = \pm 0.6$. Whilst the two outer peaks could be expected, the central peak emission needs to be studied further. Next, we compare the central and non-central peak height evolution in an NBI heated pulse (Fig. 3*(a)*): the central peak is more sensitive to NBI power, so it suggests the central peak is related to charge-exchange interaction between the NBI beam and the plasma.

We also study He II (468.6 nm) emission profiles in a pulse with NBI heating. We note the He II profile shape changes during NBI heating: the local emission for $\rho_n \geq -0.5$ is strongly increased, whereas the local emission for $\rho_n < -0.5$ is decreased (Fig. 3*(b)*).

Finally, we present a visible bremsstrahlung profile (523.5 nm) in an NBI-heated plasma ($n_e = 3.1\ 10^{-19}$ m^{-3} (averaged for $\rho_n \leq 0.5$)) and deduce the Z_{eff} profile using Eq. (2). We compare this profile with the Z_{eff} profile obtained by analysing x-ray radiation ($E_{photon} > 0.8$ keV; C and O ion emissions are supposed to be prevailing). Whereas the Z_{eff} profile deduced with x-ray emission is flat, the profile deduced with visible

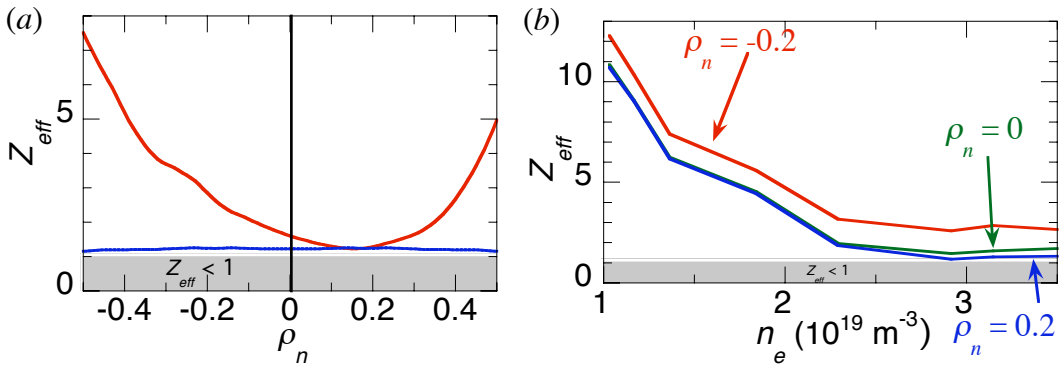

Fig. 4. (a) Comparison of Z_{eff} profiles obtained with visible bremsstrahlung (red) and x rays (blue). (b) Variation of Z_{eff} with n_e (averaged for $\rho_n \leq 0.5$).

bremsstrahlung is hollow (Fig. 4(*a*)) and its edge values are very high (they are even higher for lower densities). These high values were also found in previous Z_{eff} studies,[7,8] and suggest that other processes need to be taken into account when plasma density is low. Also, we study Z_{eff} profile variation with n_e. We observe that the central Z_{eff} is strongly decreased when n_e is high and NBI heating is working (Fig. 4(*b*)).

Conclusions

We have presented plasma emission local profiles obtained with a rotating-mirror-based system. Several problems such as the profile location, the inversion method and the local profile model were resolved. We have also studied local emission profiles and some interesting features have arisen: i.e., the profile shape depends on ion and heating type. Also, Z_{eff} has been deduced and we have found results similar to those that were previously reported. We will continue to develop this detection system with the aim of improving our characterisation of TJ-II plasmas.

References

[1] C. Hidalgo *et al.*, Nucl. Fusion **45**, S266 (2005).

[2] A. Baciero *et al.*, 30th EPS Plasma Conference (2003).

[3] M. Anton *et al.*, Plasma Phys. Control Fusion **38**, 1649 (1996).

[4] H. Meister *et al.*, Rev. Sci. Instrum. **74**, 4625 (2003).

[5] J. Herranz *et al.*, Fus, Eng. Des. **65**, 525 (2003).

[6] J. K. Anderson, Ph.D. thesis, University of Wisconsin-Madison, 2001.

[7] S. Morita and J. Baldzuhn, IPP-report (Garching, Germany) **199** (1994).

[8] J. K. Anderson *et al.*, Rev. Sci. Instrum. **74**, 2107 (2003).